# High-efficiency LED backlight optics designed with the flow-line method

Juan C. Miñano*, Pablo Benítez, Julio Chaves , Maikel Hernández, Oliver Dross, Asunción Santamaría
CEDINT, Technical University of Madrid (UPM), ETSI Telecomunicación, C. Universitaria, 28040 Madrid, Spain
Light Prescriptions Innovators. 16662 Hale Ave., Irvine, CA USA 92606

## ABSTRACT

A novel backlight concept suitable for LED's has been designed using the flow-line design method, which allows controlling both the illumination uniformity and light extraction without scattering the light. This contrasts with conventional LED backlight optical designs, which are based on the use of a light guide with Lambertian scattering features that break the guidance and extract the light. Since most of Lambertian scattered light is re-guided, the average ray path in conventional backlights is long and multiple bounces are needed, which may lead to low efficiency. On the other hand, the new design presented here is not only efficient but also provide a relatively high collimation of the output beam (an output beam within a 10 degrees half-angle cone, with total theoretical efficiency over 80% including Fresnel and absorption losses). Wider beams can be controlled by design or obtained by adding a holographic diffuser at the exit. The new design offers other very interesting practical features: it can be very thin, can be made transparent (which widens its applications, including front lighting), can mix the colors from several LED's or recover reflected polarization for LCD illumination.

**Keywords:** backlight unit, light guide plate, LED, optical design, illumination, geometrical optics

## 1. INTRODUCTION

Most existing LCDs are backlit with a cold cathode fluorescent lamp (CCFL). These lamps are efficient in terms of light output but they have some disadvantages that LEDs may overcome. Among these disadvantages are the high ignition and operation voltages, the operation at 30KHz, fragility, lengthy wait for full flux (about 10 minutes) and the use of poisonous materials, such as mercury (European Union is limiting the use of such materials). LEDs may solve some of these problems but they introduce others, such as the need for heat management, a lower efficacy (electricity to light conversion), low flux per single source, and a new light source shape. The advantages of using LEDs include their higher reliability, greater color gamut, low voltage, instant start up, higher LCD transmission for RGB LEDs, and the possibility of thinner backlights.

Typical LCD transmissions are in the range 3-8%. This means that 3-8% of the light reaching the LCD unit exits it when the LCD is in the white state. The sources of losses are many: absorptions: in the polarizers, in the color filters, pixel fill factors, and scattering. Efforts to increase the efficiency must address these factors. Most novel light guide plate designs pursue increased brightness (increasing efficiency, though sometimes reducing the emission angle) as well as thinner backlights. In References [2, 3, 4] this is achieved using different types of high quality microstructures in one or both faces of the plate.

In this paper we present a method of design of backlights structures, a method based on the control of ejected light. This control is achieved via proper design of the surfaces between which the light is guided, and the surfaces that eject the light. These guiding surfaces follow the flow lines of the bundle of the light for which it is designed. These design are done in 2D, and most of the elements of the backlight have are cylindrical solids formed by their linear sweep.

* jc.minano@ upm.es; phone +34 915441060, fax +34 915446341, www.upm.es

Following these thoughts we give an overview of the flow-line definitions and the function of etendue. The next section is devoted to explaining the beam expander, the key component of these backlights. Both backlights and front lights are described in section 3. Section 4 highlights a particular design with polarization recycling.

### 1.1 Flow line definition in 2D geometry

Let $O_1(x,y)$ and $O_2(x,y)$ be the eikonal functions of 2 bundle of rays. This means that the gradients of these functions fulfill

$$\left|\nabla O_i\right| = n(x,y) \qquad i = 1,2 \tag{1}$$

where n(x,y) is the refractive index distribution. The ray vector at the point x,y of the ray of the bundle $O_i(x,y)$ passing through this point is $\nabla(O_i)/n$. Define two more functions,

$$i(x,y) = \frac{O_1(x,y)+O_2(x,y)}{2} \qquad j(x,y) = \frac{O_1(x,y)-O_2(x,y)}{2} \tag{2}$$

the inverse functions of which are

$$O_1(x,y) = i(x,y)+j(x,y) \qquad O_2(x,y) = i(x,y)-j(x,y) \tag{3}$$

These functions fulfill that

$$(\nabla i)^2 + (\nabla j)^2 = n^2 \qquad \nabla i \cdot \nabla j = 0 \tag{4}$$

Now consider the two parameter bundle of rays *M* having $O_1(x,y)$ and $O_2(x,y)$ as edge rays (a pair of edge ray bundles $O_1(x,y)$ and $O_2(x,y)$ define two bundles: *M* and its complementary). The flow lines of *M* are defined as the lines that bisect the angle formed between the 2 edge rays. With this definition there are two possible families of edge rays. To restrict the definition next add the condition that the flow lines must be everywhere tangent to a ray of the bundle M. The lines *j*=constant, which are normal to $\nabla j$ and consequently parallel to $\nabla i$, are the flow lines of *M,* since the flow lines of M are tangent to the vector $\nabla(O_1)+\nabla(O_2)$. The lines *i*=constant are the flow lines of the complementary bundle of *M*. (see Figure 1)

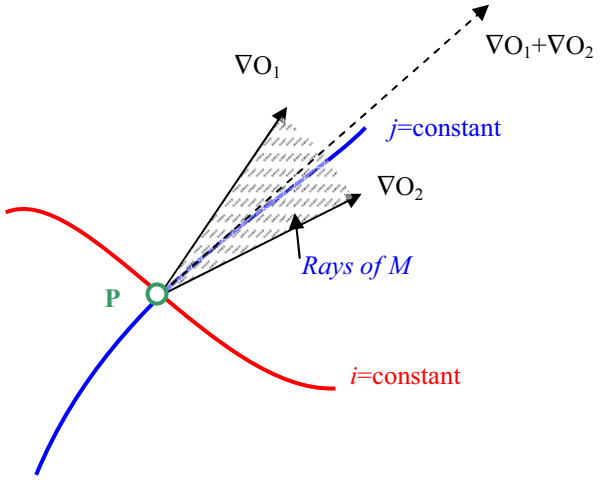


Figure 1. Iso-level lines of the functions i(x,y) and j(x,y) passing through a point P and the vectors ∇(O1), ∇(O2).

### 1.2 Stokes theorem

In 2D geometry, any ray can be fully characterized by giving the coordinates x,y of one of its points and the coordinates p,q of the tangent of the ray at this point, where p and q are the optical direction-cosines, i.e., the product of the refractive index n(x,y) times the direction cosines. These optical direction cosines must fulfil $p^2+q^2=n^2$. Consider a two-parameter bundle of rays. This set can be represented by a (two-parameter) set of points in the space x-y-p-q (restricted by the condition $p^2+q^2=n^2$), known as B. The etendue $\varepsilon_{2D}$ of a two-parameter bundle is defined as the integral of $d\varepsilon_{2D}$ over B [1]:

$$\int_B d\varepsilon_{2D} = \int_B (dpdx + dqdy) \tag{5}$$

Stokes theorem [5] establishes that the etendue $\varepsilon_{2D}$ of a 2-parameter bundle B can be calculated with a line integral along $\partial B$ (the boundary of the region B), i.e.,

$$\int_B d\varepsilon_{2D} = \oint_{\partial B} (pdx + qdy) \tag{6}$$

Consider now a 2-parameter bundle B such as the ones defined in section 1.1, i.e., such that for every point (x,y) of a certain region R of the plane x-y there are two rays which divide the rays crossing the point (x,y) in two sets: the rays belonging to B and the and the rest.

Calculate the etendue of the subset of B, defined as the rays of B that cross the open curve C, and call this subset $B_c$. $B_c$ can be defined as the rays represented by the points of the space x-y-p-q with coordinates x, y belonging to the curve C, and coordinates p, q belonging to B. The boundary of $B_c$, *i.e.*, the subset $\partial B_c$, is formed by the points of the space x-y-p-q, with coordinates fulfilling one of the following conditions

1. x,y are the coordinates of one of the edges of the curve C (points A and B, see Figure 2) and p,q belong to B
2. x,y are the coordinates of any point of the curve C, and p,q are the optical direction cosines of one of the two edge rays passing through x,y, *i.e,* (p,q)= $\nabla(O_1)$ or (p,q)= $\nabla(O_2)$

The first condition defines a subset of $\partial B_c$ that has a null contribution to the integral in Eq. (6). The contribution of the other subset defined by the second condition gives

$$\int_B d\varepsilon_{2D} = \int_C (\nabla O_1 - \nabla O_2) \cdot \mathbf{dl} \tag{7}$$

where **dl** is the differential vector (dx,dy). The minus sign comes from the two different directions of integration along the curve C when doing the line integral of Equation (6). The calculation done in Equation (6) has some subtleties about the direction in which we have to do the line integral (see reference [5]) and also regarding the direction of the edge rays. Note that the vector fields $\nabla(O_1)$ and $\nabla(O_2)$ define exactly the same edge rays as $-\nabla(O_1)$ and $-\nabla(O_2)$, respectively. Only the direction of progression of the rays is different. In order to simplify this problem, impose the requirement that vector fields $\nabla(O_1)$ and $\nabla(O_2)$ must have the directions such that the vector $\nabla(O_1)+\nabla(O_2)$ is parallel to some (p,q) that belongs to B. Also we establish that the integral in equation (7) is done from the edge of C with the lowest value of the function j.

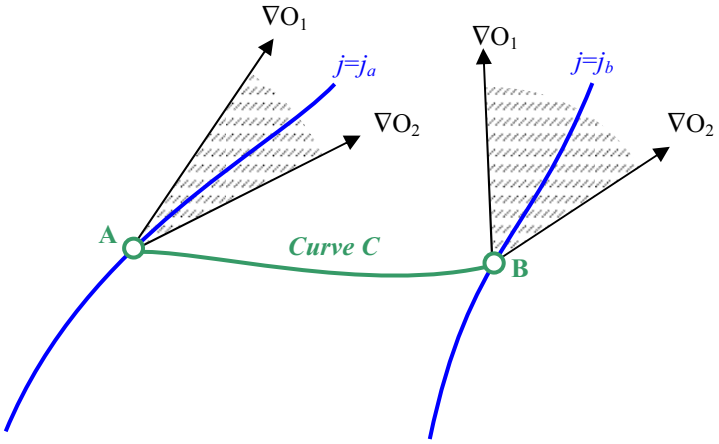


Figure 2. Rays of the bundle $B_s$.

Assuming that this edge point is A we have

$$\int_B d\varepsilon_{2D} = 2(j(x_B, y_B) - j(x_A, y_A)) \tag{8}$$

i.e., the etendue of $B_c$ is twice the difference between the value of the function j(x,y) at both curve extremes. The difference between the value of the function i(x,y) at both curve extremes is proportional to the etendue of the subset of

the complementary bundle of B that crosses the curve C. If the curve C is the differential vector **dl**, then the differential of etendue $d\varepsilon_{2D}$ of the bundle of rays of B crossing **dl** equals 2dj.

### 1.3 Example: Finite radiating strip

Consider the bundle of rays $B_s$ emanating from the strip of the y axis limited by $P_1$ and $P_2$ and such that the angle of the rays with respect the x axis is smaller than $\alpha$. The refractive index is assumed equal to 1 everywhere. The edge ray bundle is formed by the rays shown in Figure 3. This edge ray bundle is of the type mentioned in Section 1.1, *i.e.*, there is a region of the x-y plane such that every point of this region is crossed by two edge rays (this region is bounded for $x \geq 0$ by the rays $r_1$ and $r_2$). One of the edge rays belongs to the subset drawn at the left of Figure 3 and the other belongs to the subset drawn at the right hand side. There are no rays of the bundle outside this region.

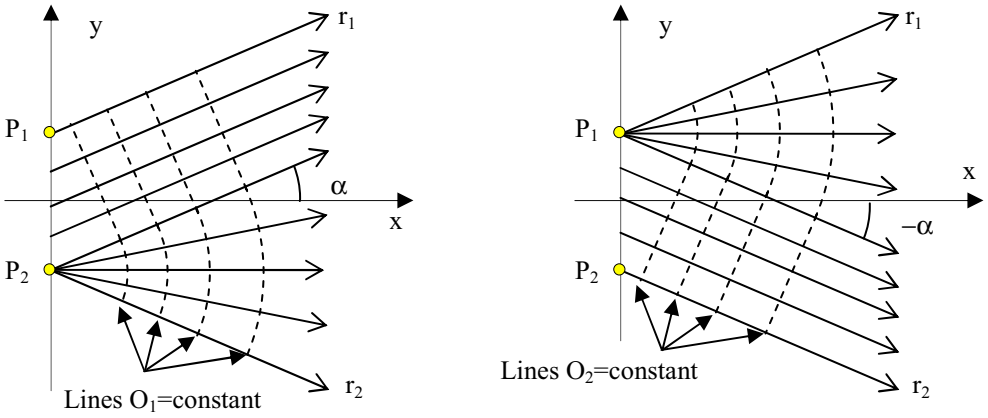


Figure 3. Edge rays of the beam radiating from the strip $P_1$-$P_2$ at angles restricted to $\pm\alpha$.

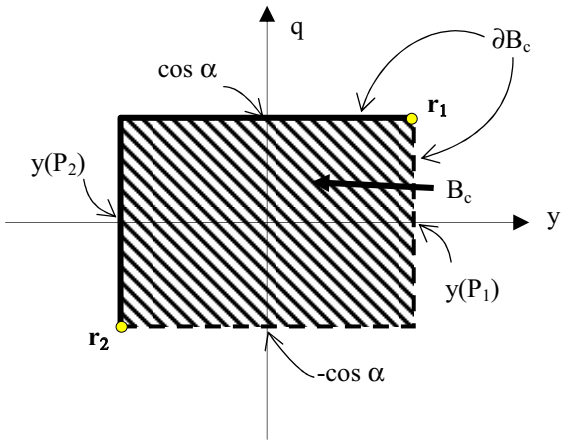


Figure 4 Phase space representation of $B_s$ when x=0 showing the edge rays $r_1$ and $r_2$, having the trajectory in the configuration space x-y, as shown in Figure 3. The bounding edge-ray bundle ∂Bs is represented by the points of the contour of this rectangle. The continuous line represents the edge ray on the left hand side of Figure 3 and the dotted line represents the rays of the right side.

Figure 4 shows the phase-space representation of the beam, the edge rays of which are those of Figure 3. The coordinates y-q of each ray are calculated at x=0. The contour of this region represents the edge rays, among which are the rays $r_1$ and $r_2$, which are marked with a dot in this Figure. Note that these two rays separate the two subsets of edge rays, *i.e.*, we can consider that they belong to both subsets. Consequently, their trajectory is also the trajectory of a flow line.

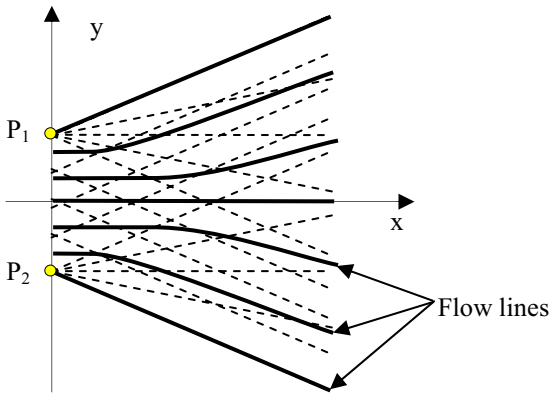


Figure 5. Flow lines for the beam radiating from the strip $P_1$-$P_2$ at angles restricted to $\pm\alpha$. The edge rays are shown as dotted lines

Figure 5 shows the flow lines for the beam whose edge rays are those of Figure 3. These flow-lines are the lines j=constant. Figure 6 shows an element of a curve that intercepts a differential amount of etendue, equal to $2\Delta j$ according to equation (8). When the curve element is coincident with a flow line, the amount of etendue intercepted is zero. This is because the etendue intercepted by one face of the curve element cancels out the etendue intercepted by the other face. The reason for this cancellation is easy to see: the bundle is locally symmetric with respect to the tangent to the flow line. Because of this symmetry, a mirror placed along a flow line does not disturb the bundle because it reflects exactly the same rays that it blocks [1].

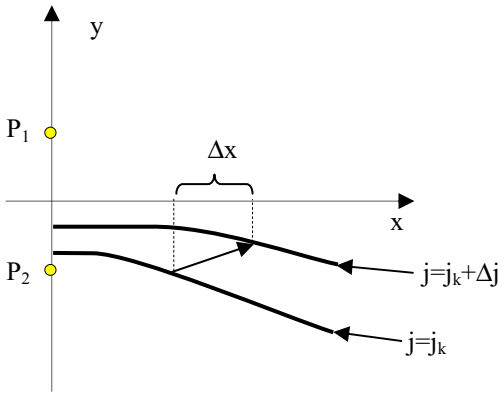


Figure 6. The etendue intercepted by the differential element is twice $\Delta j$

## 2. BEAM EXPANDERS

The beam expander constitutes the core element of the backlights shown herein. It is a piece for which the function is to "slice" the incoming bundle into small "light ribbons", which are ejected perpendicularly from the beam expander. Additionally, the beam expander can also collimate the light. Figure 7 shows the cross section of a generalized beam expander. This beam expander cross section is bounded by an entrance through which the light enters into the beam expander, in general after some collimation; as well as by a deflector line and a microstructured line.

The refractive index is assumed to be about 1.5 inside these boundaries, and 1 outside them (unless something else is specified). The deflector line has the shape of a flow line of the bundle entering into the beam expander. The rays of the bundle are assumed to have narrow enough collimation such that all are totally internally reflected when they hit any flow line. The microstructured line is a line formed by two alternating types of segments, one of which is called the ejector. These ejectors reflect the light impinging on them and send it towards the deflector line. The ejector line is close to a horizontal straight line, and the ejector segments are close to the 45-degree tilted segments. The light reflected by the ejectors reach the deflector line almost perpendicularly, so that this light is refracted outside the beam expander. The other type of segment is either a flow line or an arbitrary line located in the shadow region generated by the ejectors, *i.e.*, located where the rays of the bundle cannot intercept it.

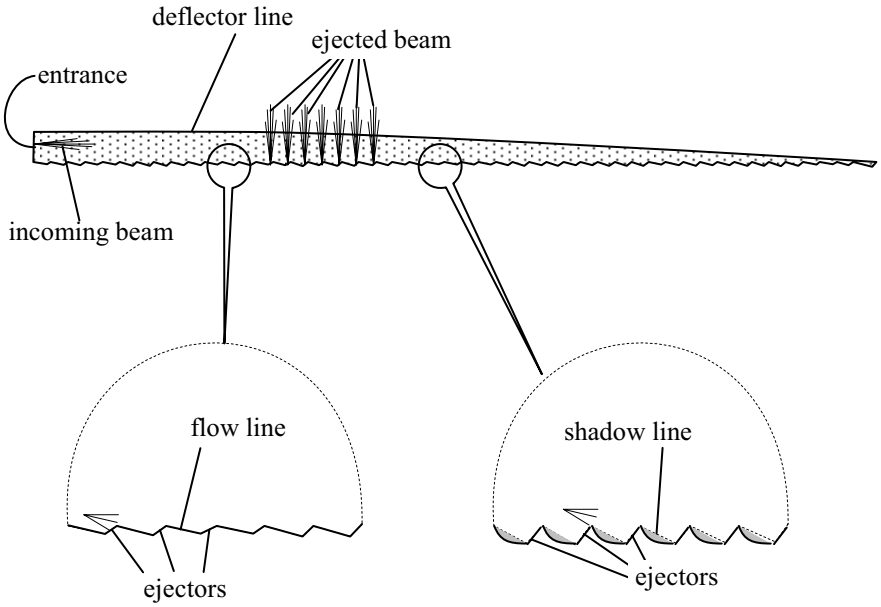

Figure 7. Beam expander cross-section showing two types of microstructured line.

Consider the first case, in which the segments in between ejectors are flow lines. Each ejector is connecting two flow lines. Assume that the difference between the j of both lines is $\Delta j$. Then, the etendue of the ejected bundle slice is $\Delta\varepsilon_{2D}=2\,\Delta j$. The bundle of rays remains unaffected after the ejection of this slice, excepting that it contains one slice less, but the edge rays of the remaining bundle are the same as they were before the ejection. This is because each of the deflections suffered by the rays is either a reflection at a flow line (which do not disturb the bundle [1]) or a reflection that ejects the rays from the beam expander (and thus these rays are not proceeding anymore inside the beam expander). When the segments between ejectors are lines located in the shadow region generated by the ejectors, the same assertion holds, *i.e.*, after each light slice ejection, the bundle of rays remains unaffected excepting that it contains one slice less. In this case, the lines in between ejectors do not intervene because they are not "seen" by the bundle.

Each ejector is consuming a small amount of etendue, until the last ejector has exhausted all the available etendue. Assume that $j_0$ and $j_1$ are the values of j for the two edges of the beam expander entrance, in particular, assume that $j_1$ ($j_1 > j_0$) is the value corresponding to the deflector line. Each ejector jumps an amount $\Delta j$ (which may be different for different ejectors) until the last ejector gets the line $j=j_1$.

Assuming that the rays of the bundle have a constant normalized radiance ($\Re=1$), then the light power contained in each slice is $\Delta\varepsilon_{2D}$. A design extracting the same amount of power per ejector must have a constant $\Delta j$ jump for each ejector. The total number of ejectors would be $(j_1 - j_0)/\Delta j$. If additionally we need the ejectors to be equally spaced in the x direction, then the x increment between two consecutive ejectors will be $\Delta x = L\ \Delta j\ /(j_1 - j_0)$ (see Figure 6). When $\Delta j \to 0$ the microstructured curve (but not its derivative!) tends to the curve satisfying the differential equation

$$\frac{dj(x,y)}{dx} = \text{constant} \tag{9}$$

where y(x) is the unknown function. One simple and special case is found when the two sets of edge rays are formed by parallel rays, i.e., when $P_1$ and $P_2$ of Figure 3 are infinitely far away from the x axis. In this case the function j(x,y) is proportional to y (i.e., the flow lines are lines parallel to the x axis) and the result of Eq. (9) gives a straight line. This case will be called the linear beam expander.

Figure 8 shows how to calculate the microstructured line once the input bundle is known. Firstly, the flow lines are calculated. In the case of Figure 8, the input bundle is formed by the rays crossing the segment $P_1$-$P_2$ forming an angle with the x axis between $\pm\alpha$. Assume that $P_1$ and $P_2$ are symmetric with respect the x axis. Then the x axis is a flow line. We choose this straight line as the deflector line. The microstructured line is started at some point between $P_1$ and $P_2$ (which fits with the available etendue) by taking out small portions of the flow line until $\Delta x$ attains the desired value. Then the tilted portion of the ejector is designed to reflect the light outside the beam expander. This ejector design must take into account the refraction at the deflection line (in this example this refraction is very simple because the deflection line is straight). The ejector produces an additional $\Delta x$, which must be taken into account in the design, although it is negligible in general. The ejector is extended until it finds the flow line whose j is $+\Delta j$ greater.

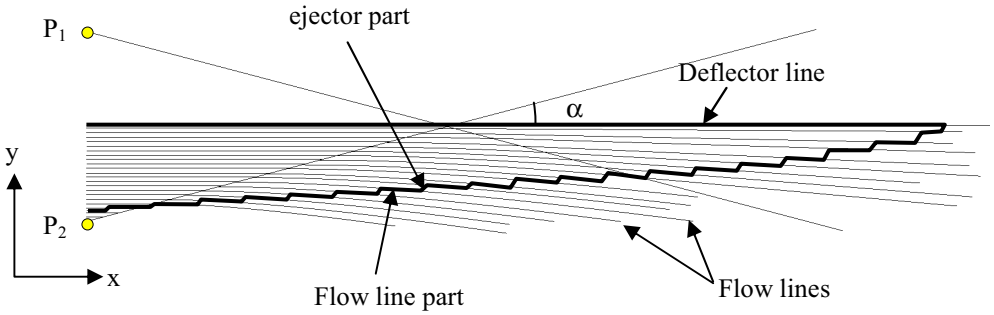


Figure 8. The microstructured line is build up with parts of flow lines and parts

The microstructured line progresses along this flow line. The procedure is repeated until the microstructured line finds the deflection line. If the microstructured line is of the second type, shown in Figure 7, then the design is not yet finished. For this type of microstructured line it is necessary that any ray being reflected at the flow line portions find the corresponding next ejector immediately after the reflection. This guarantees that extracting the flow line portion will only affect the light being reflected by the next ejector and so this extraction will not modify the bundle elsewhere. The design procedure continues, taking out all the flow line portions of the microstructured line and calculating the shadow lines. The ejectors are extended back until they find the shadow lines. The lines linking consecutive ejectors can be chosen freely in the shadow region. These ejector structures were studied previously by Chaves [6] for ultra thin solar energy concentrators.

To have the beam expander completely surrounded by optically active surfaces can be a manufacturing problem sometimes. A bundle of rays can be chosen such that the flow line corresponding to the deflection line coincides totally or partially with a caustic. In this case, there is no need to have a reflecting surface in the part of the deflection line that coincides with the caustic, because in the caustic the rays of both subsets of edge rays are the same (the case drawn in Figure 3 can be viewed as a limit case in which the caustic contains only one ray $r_1$ or $r_2$).

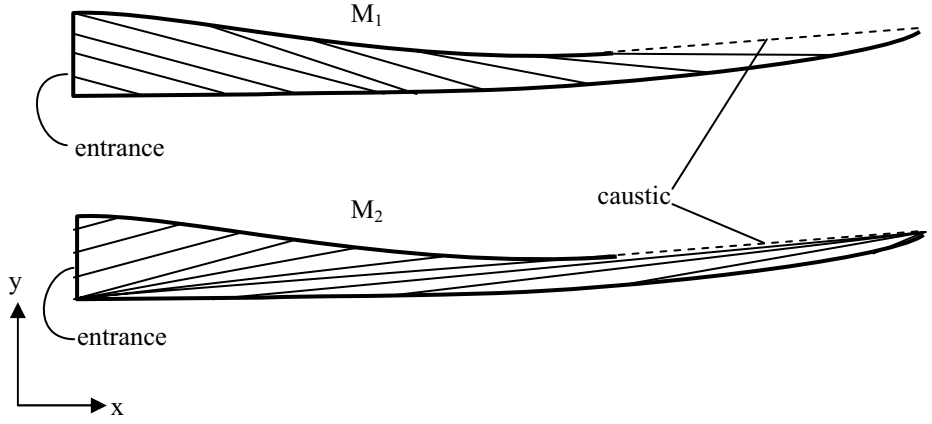

Figure 9. These 2 subsets of edge ray bundles share the rays of the caustic (dashed line).

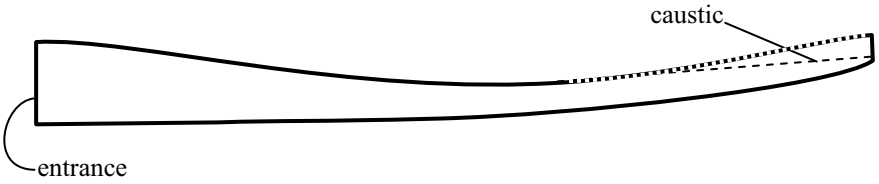


Figure 10. The upper surface of the beam expander has a portion not coincident with the flow line

## 3. BACKLIGHTS

Figure 11 shows one possible case of backlight in which two beam expanders are combined. For the sake of clarity, let us assume that the light source is a rectangle of 1.8 mm ($D_y$) times 0.45 mm ($D_z$) in air (refractive index 1). This is for instance the size of the emitting area of the Nichia's LED NSCW020. The beam expander thickness $h_z$ (z axis), the angular spread at the collimators exit aperture in the x-z plane $\theta_{zx}$, the y axis side length of the illuminated area $L_y$ and the z axis length $D_z$ of the emitting area are related by the following equations (derived from the etendue $\varepsilon_{2D}$ conservation) in the configuration of Figure 11.

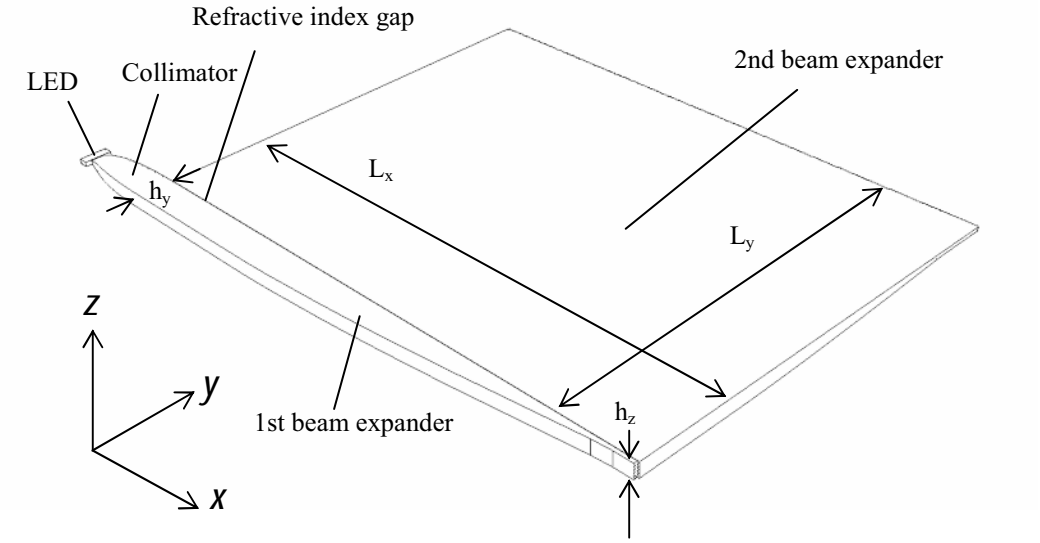


Figure 11. Two beam expanders are combined to get a lighting unit which can be used as a backlight or as a frontlight

$$\begin{aligned} \varepsilon_{2D} &= 2D_{zx} \\ \varepsilon_{2D} &= n\, L_y\, (1-\cos\theta_{zx}) \\ \varepsilon_{2D} &= 2n\, h_z\, \sin\theta_{zx} \end{aligned} \tag{10}$$

Consider a refractive index $n = 1.59$ and $L_y = 55.25$ mm, then the equations result in in $\theta_{zx} = \pm 8.21$ deg, and $h_z = 1.98$ mm. In Equations (10) it was implicitly assumed that $L_y >> h_z$ and that the microstructured line is illuminated from grazing angles (0 deg) until $\theta_{zx}$ .or, what is the same, it has been assumed that the microstructured line is parallel to the x axis, and with the same y coordinate as the point $P_2$, and assumed that the y coordinate of $P_1$, $y(P_1)$ is far away, so that $y(P_1)/\tan\theta_{zx} > L_y$. With these results, the ejectors of the second beam expander can work by total internal reflection (TIR), so that no metalization is needed on this beam expander. The area of the ejectors projected on the xy plane, relative to the the projected area of the second beam expander, is $h_z/L_y = 3.6\%$. This means that the second beam

expander is almost transparent when seen normal to the aperture (the refractions can be corrected with an additional transparent piece if necessary). This enables it to be a front light illuminator.. In this configuration, the beam expander is in between the observer and the LCD, which must be reflexive type. The first beam expander maximum width $h_y$ and the angular spread $\theta_{xy}$ are given by similar equations in the transverse axes

$$\begin{aligned} \varepsilon'_{2D} &= 2D_y \\ \varepsilon'_{2D} &= n\, L_x\, (1-\cos\theta_{xy}) \\ \varepsilon'_{2D} &= 2n\, h_y\, \sin\theta_{xy} \end{aligned} \tag{11}$$

For $L_x$= 73.67 mm it results in $\theta_{xy}$=±14..24 deg, and $h_y$=4.6 mm. The internal angles $\theta_{zx}$ and $\theta_{xy}$ result in an angular spread of ±13.12 deg (plane xz) and ±23.03 deg (plane yz) for the radiation escaping from the second beam expander. A diffuser after the second beam expander can be introduced to increase this angular spread.

As shown in Figure 11 the first and second beam expanders are glued with a material having a refractive index smaller than the refractive index n of the first beam expander. In this way, the deflection surface of the first beam expander reflects the rays coming from the collimator. The refractive index of the glue $n_g$ must fulfill that $n_g < n \cos\theta_{xy} = 1.54$. Another solution consists of using a second beam expander material with a refractive index smaller than 1.54. Neither solution is difficult to accomplish, although the second requires consequent changes to the entire second beam expander.

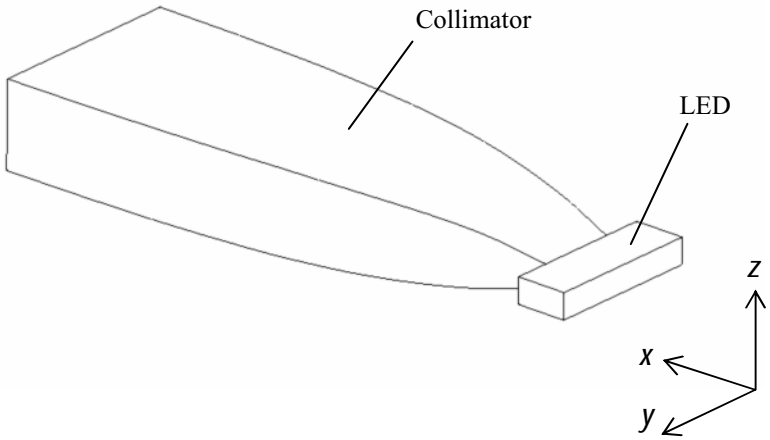


Figure 12. Cross CPC collimator

In order to use TIR for guiding the light, it must enter the beam expander with some collimation. The minimum collimation needed can be easily achieved (sometimes with a simple refraction at a flat surface). If in addition to getting uniform irradiance at the output plane of the second beam expander, the angular emission angle must be nearly uniform at the same output plane, then the light entering the first beam expander must be substantially collimated, *i.e.*, with an angular spread similar to that desired for the output beam. In this case, a collimator before the first beam expander is recommended. Figure 12 shows a view of the collimator, which in this case is a cross-CPC.

## 4. POLARIZATION RECICLYNG

One of the main sources of losses in an LCD backlight system comes from the need for polarized light. If the light with the unwanted polarization is not recycled, then these losses are at least 50% of the incoming (unpolarized) light. Such significant losses have impelled ideas for increasing the LCD backlight efficiency (see for instance [7]).
We can take advantage of some of the properties of the beam expander to recycle the unwanted polarization in a simple way.
Figure 13 shows the cross section of a beam expander with polarization recycling.

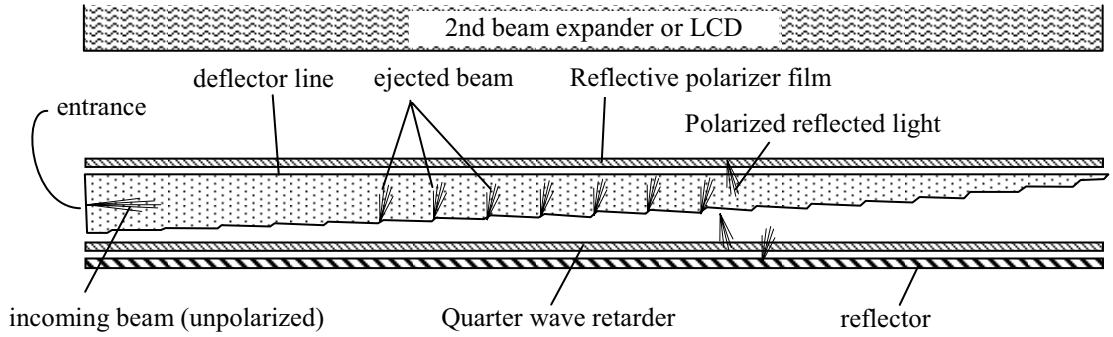


Figure 13. Cross-section of the backlight system with polarization recovery

The beam expander concept works by slicing the bundle into small light strips (perhaps a most adequate name would be beam slicer). Expanding the beam, which would produce a smaller emission angle, is not necessary, although this can be done at the same time. As the beam is sliced, there are alternated shadow strips in the emission area. These strips, which typically are much wider than the light strips, can be used to recycle the unwanted polarization. The light ejected by the beam expander is slightly tilted with respect to the normal to the reflective polarizer film that is placed in front of the beam expander aperture. An example of such film is that referenced in [8, 9] DBEF-P2 films in which the desired polarization filter characteristics are achieved by a clever use of birefringent films. Because the ejected beam is slightly tilted, the unwanted reflected polarization finds the shadow strips when it crosses back over the microstructured line. This allows this light to cross the beam expander and to find a quarter-wave retarder plus a reflector that sends back the light, now with the desired polarization, through the shadow strips. As a result, the unwanted polarization is recycled, and the number of light strips is doubled. If in addition the beam expander is linear, then it can be combined with another one injecting light from the right hand side, as shown in Figure 14 providing color mixing if necessary.

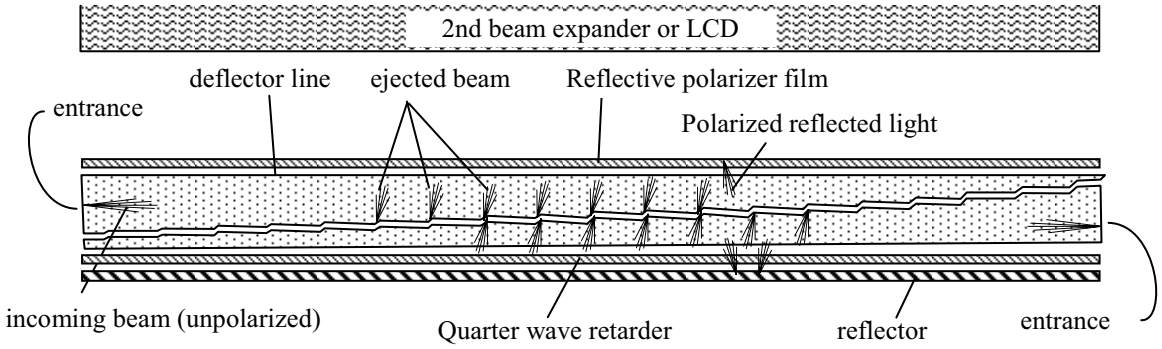


Figure 14. Cross-section of the backlight system with polarization recovery and double injection

This polarization recycling scheme can be used in the first or the second beam expanders. Using it in the first beam expander requires less area for the reflective polarizer, quarter wave retarder and reflector films, which has obvious advantages, and also allows front or backlighting. Figure 15 shows the other case, in which the polarization recycling is done in the second beam expander, and in which case only backlighting is possible.

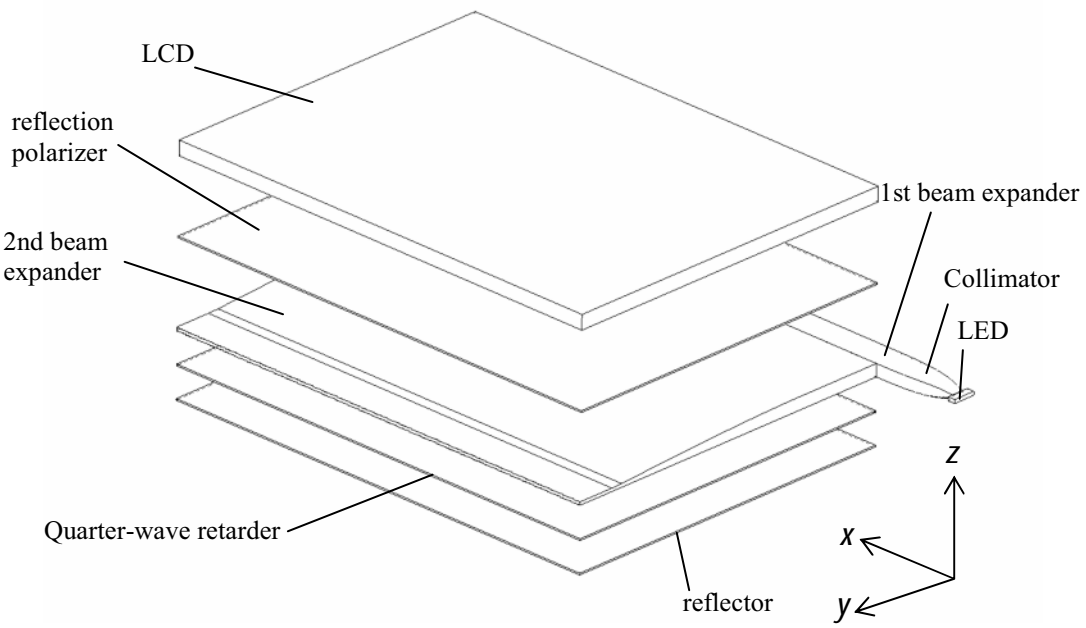


Figure 15. Backlight with polarization recovery

## 5. CONCLUSIONS

A novel backlight design based on the flow line method has been present. The new design contains a basic piece called the beam expander which guides the beam in between flow lines and periodically ejects a part of it creating an output beam which is formed by small ribbons of light. A proper design gets the guiding by TIR and consequently, the light guide is almost transparent as seen from the observer since the ejectors occupy a small fraction of the exit aperture. This feature can also be used to recycle polarized light or to mix colors.

## 6. ACKNOWLEDGMENTS

This work has been funded by the Spanish Ministry of Science and Education (project TEC2004-04316) and the Commission of the European Communities under contract TSTE-CT-2003-506316 (ISLE). The authors thank Bill Parkyn for his help in editing the paper.

## 7. LEGAL NOTICE

The devices and configurations described herein are the subject of a United States Patent Pending.

## 8. REFERENCES

1. R. Winston, J.C. Miñano, P. Benítez, “Nonimaging Optics”, Elsevier, Academic Press, 2004
2. K. Käläntär, S. Matsumoto, and T. Onishi, “Functional light-guide plate characterized by optical microdeflector and micro-reflector for LCD backlight”, IEICE TRANS. ELECTRON., E84-C, 1637-1646 (2001).
3. Di Feng, Yingbai Yan, Xingpeng Yang, Guofan Jin and Shoushan Fan, “Novel integrated light-guide plate for liquid crystal display backlight”, J. Opt. A: Pure Appl. Opt., 7, 111–117 (2005).
4. Di Feng, Guofan Jin, Yingbai Yan, Shoushan Fan, “High quality light guide plates that can control the illumination angle based on microprism structures”, Applied Physics Letters, 85, 6016-6018 (2004).
5. H. Flanders, “Differential Forms with Applications to the Physical Sciences”, Dover, New York, 1989
6. Julio Chaves. "New contributions for nonimaging optics or anidolic optics" Dissertation for obtaining the Ph. D. degree in Technological Physics Engineering, Instituto Superior Tecnico Lisbon, Portugal, September 2002.

7. H. Tanase, J. Mamiya, M. Suzuki, “A new backlighting system using a polarizing light pipe” IBM J. res. Develop. Vol. 42 no. ¾ pp 527- 536 (1998)
8. M. F. Weber, C.A. Stover, L.R. Gilbert, T.J. Nevitt, A.J. Ouderkirk, “Giant Birefringent Optics in Multilayer Polymer Mirrors”, Science, 287, March 2000, pp 2451-2456
9. S. Eckhardt, C. Bruzzone, D. Aastuen, J. Ma “3M PBS for High Performance LCOS Optical Engine”, http://multimedia.mmm.com/mws/mediawebserver.dyn?8888882dpil8r0y8K0y888S8SIsBcsRD-